Acta Crystallographica Section F
Structural Biology Communications
ISSN 2053-230X

Cloning, purification, crystallization and 1.57 Å resolution X-ray data analysis of AmsI, the tyrosine phosphatase controlling amylovoran biosynthesis in the plant pathogen *Erwinia amylovora*

Stefano Benini,[a]* Lorenzo Caputi[b] and Michele Cianci[c]

[a]Laboratory of Bioorganic Chemistry and Bio-Crystallography (B_2Cl), Faculty of Science and Technology, Free University of Bolzano, Piazza Università 5, 39100 Bolzano, Italy, [b]Biological Chemistry Department, John Innes Centre, Norwich Research Park, Colney, Norwich NR4 7UH, England, and [c]EMBL, Notkestrasse 85, 22607 Hamburg, Germany

Correspondence e-mail: stefano.benini@unibz.it

Received 10 October 2014
Accepted 13 November 2014

The Gram-negative bacterium *Erwinia amylovora* is a destructive pathogen of plants belonging to the Rosaceae family. Amongst its pathogenicity factors, *E. amylovora* produces the exopolysaccharide amylovoran, which contributes to the occlusion of plant vessels, causing wilting of shoots and eventually resulting in plant death. Amylovoran biosynthesis requires the presence of 12 genes (from *ams*A to *ams*L) clustered in the *ams* region of the *E. amylovora* genome. They mostly encode glycosyl transferases (AmsG, AmsB, AmsD, AmsE, AmsJ and AmsK), proteins involved in amylovoran translocation and assembly (AmsH, AmsL and AmsC), and also a tyrosine kinase (AmsA) and a tyrosine phosphatase (AmsI), which are both involved in the regulation of amylovoran biosynthesis. The low-molecular-weight protein tyrosine phosphatase AmsI was overexpressed as a His_6-tagged protein in *Escherichia coli*, purified and crystallized. X-ray diffraction data were collected to a maximum resolution of 1.57 Å in space group $P3_121$.

1. Introduction

Erwinia amylovora is a Gram-negative bacterium belonging to the Enterobacteriaceae family. It causes the devastating disease called fire blight in Rosaceae such as apple, pear, raspberry, cotoneaster and pyracantha (Vanneste, 2000). *E. amylovora* infects the host plants during spring, primarily in the flowers through the nectarthodes, or during summer, attacking the succulent tissues of shoots through wounds caused by hail, wind, storms and insects. Once established in the plant, the bacteria move through the vascular system of the plant, spreading the infection to other tissues and escaping the plant defence with the help of a capsular exopolysaccharide (EPS), which also represents one of the most important pathogenicity factors of *E. amylovora* (Vrancken *et al.*, 2013). The EPS causes occlusion of the plant vessels, resulting in the characteristic wilting of fire blight, and eventually leading to plant death (Gross *et al.*, 1992). The EPS of *E. amylovora* contains two different types of sugar polymers, amylovoran and levan, that are essential to biofilm formation, which in turn protects the bacteria and helps to spread the disease. Δ*ams* mutants defective in the synthesis of amylovoran were nonpathogenic, while Δ*lsc* mutants defective in the synthesis of levan did not colonize xylem vessels and only moved slowly into apple shoots (Koczan *et al.*, 2009). Levan is a fructo-oligosaccharide synthesized by the action of a single enzyme, levansucrase (Geier & Geider, 1993; Caputi, Cianci *et al.*, 2013; Caputi, Nepogodiev *et al.*, 2013), while the biosynthesis of the long-chain amylovoran requires a complicated enzymatic system. Amylovoran is a repetition of oligosaccharide units of galactose, glucose, glucuronic acid and pyruvate (Nimtz *et al.*, 1996). EPS biosynthesis, regulation and secretion involves the action of 12 genes clustered in the 16 kb *ams* region (from *ams*A to *ams*L) in the *E. amylovora* genome (Bugert & Geider, 1995). Most of them are glycosyl transferases (AmsG, AmsB, AmsD, AmsE, AmsJ and AmsK); the other proteins are involved in amylovoran translocation and assembly (AmsH, AmsL and AmsC) and include a tyrosine kinase (AmsA) and a tyrosine phosphatase (AmsI) that are both involved in regulating the production of amylovoran (Langlotz *et al.*, 2011). The biosynthesis of amylovoran is regulated by a network of proteins which includes the phosphorelay system RcsB, RcsC and

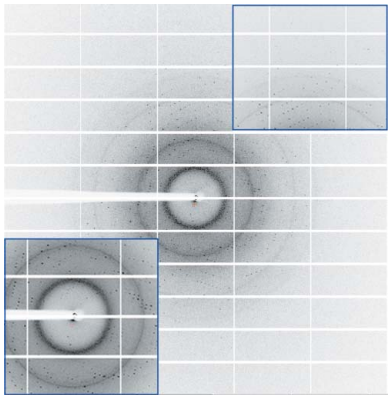

Table 1
Macromolecule-production information.

Source organism	*E. amylovora* strain Ea273 (ATCC 49946)
DNA source	Genomic
Forward primer	5′-CGATCACCATGGTCAATTCAATCTTAGTGG
Reverse primer	5′-CGAGAATTCCTATCGGCTTAATGCG
Cloning vector	pETM-11
Expression vector	pETM-11
Expression host	*E. coli* BL21 (DE3)
Complete amino-acid sequence of the construct produced†	MKHHHHHHPMSDYDIPTTENLYFQGAMVNSILVVCIGNICRS-PTGERLLKAALPERKIASAGLKAMVGGSADETASIVANEH-GVSLQDHVAQQLTADMCRDSDLILVMEKKHIDLVCRINPS-VRGKTMLFGHWINQQEIADPYKKSRDAFEAVYGVLENAAQ-KWVNALSR

† The AmsI sequence is underlined.

RcsD (Wang *et al.*, 2009, 2011) and the recently characterized negative regulator of amylovoran production AmyR (Wang *et al.*, 2012).

AmsI, a protein tyrosine phosphatase (EC 3.1.3.48), was initially proposed to be a low-molecular-weight phosphatase (144 amino acids, molecular mass of 15 772.2 Da as calculated by *ProtParam* from ExPASy) used to dephosphorylate lipid carrier diphosphates during amylovoran assembly (Bugert & Geider, 1997). AmsI was later proposed to act in concert with AmsA, a tyrosine kinase associated with the production of exopolysaccharide (Ilan *et al.*, 1999) and located downstream of the AmsI gene in the *ams* operon (Bugert & Geider, 1995). AmsA and AmsI are homologues of Wzc and Wzb, respectively, in *Escherichia coli*, which regulate colanic acid production. In *E. coli* the interplay between the autokinase Wzc and Wzb regulates colanic acid synthesis by changing the phosphorylation state of Wzc by the action of Wzb. The bacteria only produced colanic acid when the autophosphorylated Wzc is dephosphorylated by Wzb (Vincent *et al.*, 2000). The structure of Wzb was solved by NMR and provided the evidence for a substrate-recognition mechanism that differs from that of eukaryotic tyrosine phosphatases, suggesting that Wzb could represent an ideal target for structure-based drug design to fight pathogenic bacteria (Lescop *et al.*, 2006). We cloned, overexpressed, purified and crystallized AmsI. The structural data collected to 1.57 Å resolution will help towards a better understanding of the mechanism of its interaction with AmsA and drive the development of inhibitors able to eradicate fire blight.

2. Materials and methods

2.1. Cloning, overexpression and purification of *E. amylovora* AmsI

The *ams*I gene (UniProt Q46630) was PCR-amplified from genomic DNA isolated from *E. amylovora* strain Ea273 (ATCC 49946). The forward and reverse primers included *Nco*I and *Eco*RI restriction sites, respectively (underlined in Table 1). The PCR product was purified, digested for 3 h at 310 K and ligated into pETM-11 vector (Dümmler *et al.*, 2005). The obtained plasmid (pETM-11::AmsI) was propagated in *E. coli* NovaBlue cells (EMD4 Biosciences, Germany). *E. coli* BL21 (DE3) cells were transformed with pETM-11::AmsI for expression of the recombinant His_6-tagged protein. Table 1 reports the details of the cloning procedure. After initial small-scale expression trials, which demonstrated good levels of protein expression, the transformed cells were grown overnight in 10 ml 2×YT medium containing kanamycin (30 µg ml^{-1}) at 310 K. The culture was used to inoculate 1 l medium (1:100 dilution) and grown at 310 K to an OD_{600} of 0.8. The temperature was then decreased to 293 K and after 1 h the culture was induced with 1 m*M* IPTG and grown for a further 16 h. The cells were harvested by centrifugation at 4500*g* for 15 min at 277 K, washed with 100 ml ice-cold 50 m*M* sodium phosphate pH 7.4, 250 m*M* NaCl, 0.5 m*M* TCEP (buffer *A*) and centrifuged again, yielding 6 g of wet cell paste. The cells were resuspended in 50 ml buffer *A* containing 0.2 mg ml^{-1} lysozyme and a protease-inhibitor tablet (Roche, Switzerland), stirred for 30 min at room temperature and lysed by sonication (Soniprep, MSE, UK) on ice for 2 min using 10 s cycles (15.6 MHz) and a 9.5 mm diameter probe. Cell debris was removed by centrifugation at 18 000*g* for 20 min at 277 K. After filtration through a 0.45 µm cellulose acetate filter, the cell extract was loaded onto a HisTrap HP 5 ml column (GE Healthcare, Sweden) previously equilibrated with buffer *A* at a flow rate of 2 ml min^{-1}. The column was then washed with buffer *A* supplemented with 20 m*M* imidazole until the A_{280} reached the baseline. An imidazole gradient from 20 to 500 m*M* in buffer *A* for 20 column volumes (100 ml) was applied and the enzyme eluted at a concentration of 150 m*M* imidazole. The fractions containing the enzyme were pooled, concentrated by ultrafiltration using a Vivaspin 20 (Sartorius) and loaded onto a Sephadex S75 16/60 column (1.6 × 60 cm; GE Healthcare, Sweden) equilibrated with 20 m*M* Tris–HCl pH 7.5, 150 m*M* NaCl, 0.5 m*M* TCEP (buffer *B*) at a flow rate of 1 ml min^{-1} (Fig. 1). All purification steps were carried out at room temperature. Protein purity was confirmed by SDS–PAGE.

Table 2
Crystallization.

Method	Microbatch under oil
Plate type	96-well MRC plates
Temperature (K)	293
Protein concentration (mg ml^{-1})	15
Buffer composition of protein solution	20 m*M* Tris–HCl pH 7.5, 150 m*M* NaCl, 0.5 m*M* TCEP
Composition of reservoir solution	1.7 *M* ammonium sulfate, 100 m*M* sodium acetate pH 5.5
Volume and ratio of drop	1 µl, 1:1

2.2. Crystallization

The protein was crystallized using the microbatch-under-oil method in 96-well MRC plates. The crystallization wells were protected from drying using adhesive ClearView sheets (Molecular Dimensions). Drops of 1 µl precipitant solution from the crystallization kits [PACT *premier* HT-96 and JCSG-*plus* HT-96, CSS1 and CSS2 (Brzozowski & Walton, 2001); Molecular Dimensions] were

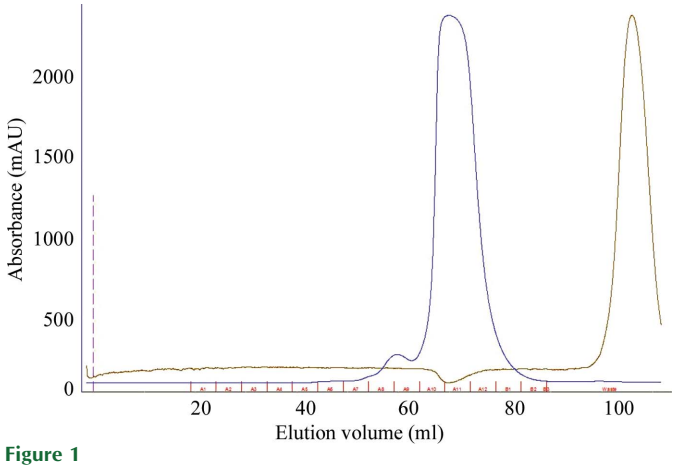

Figure 1
Elution profile of the size-exclusion chromatography carried out as a second step of the purification using a Sephadex S75 16/60 column (1.6 × 60 cm; GE Healthcare, Sweden). The injection volume was 5 ml protein solution (the blue line represents the UV absorption at 280 nm). This step was used as a desalting step as well (the brown line represents the conductivity of the solution).

added to 15 µl volatile oil (Molecular Dimensions) using a multichannel pipette, immediately followed by 1 µl protein solution. A shower of very small crystals appeared within a week in condition A7 of the CSS2 screen (2.7 *M* ammonium sulfate, 100 m*M* sodium acetate pH 5.5). The conditions were replicated using a grid of different ammonium sulfate concentrations and crystals grew to a maximum size of about 0.2 × 0.2 × 0.2 mm in 1.7 *M* ammonium sulfate, 100 m*M* sodium acetate pH 5.5. A summary of crystallization is provided in Table 2. A crystal was scooped from the mother liquor using a cryoloop and flash-cooled at the beamline by quickly mounting it onto the goniometer straight into the nitrogen stream of the cryocooling system to test its diffraction properties. The high-salt mother liquor and the tiny layer of surrounding oil around the crystal provided good cryoprotection, allowing the collection of a complete high-quality data set (Table 3).

2.3. Data collection and processing

Diffraction data were collected at 100 K on the EMBL P13 beamline at the PETRA III storage ring, DESY, Hamburg, Germany. The wavelength was set to 1.033 Å using a Si(III) crystal monochromator (FMB Oxford). Data were collected with a focused beam collimated with a 70 µm diameter aperture using a PILATUS 6M detector (DECTRIS) and an MD2 goniometer (Maatel-EMBL) with a horizontal spindle axis. The data were processed using *XDS* (Kabsch, 2010), the space group was determined by *POINTLESS* (Evans, 2011) and the data were scaled with *AIMLESS* (Evans, 2006). The crystal diffracted to 1.57 Å resolution in space group $P3_121$. Data-collection statistics are reported in Table 3.

3. Results and discussion

The *E. amylovora* AmsI gene was amplified from genomic DNA and ligated into pETM-11 expression vector. His_6-tagged AmsI was overexpressed in *E. coli*, yielding 80 mg protein per litre of culture. Crystals of AmsI grew from a two-step protein-purification protocol without removing the His_6 tag from the protein and using microbatch under oil, thus facilitating their transport to the beamline. The crystal of AmsI used for data collection belonged to space group $P3_121$ and diffracted to 1.57 Å resolution (Fig. 2) without addition of cryoprotectant to the microbatch-under-oil crystallization conditions. The asymmetric unit contains one molecule of AmsI with a solvent content of 55.36% and a Matthews coefficient of 2.75 $Å^3$ Da^{-1}. The structure will be solved by molecular replacement using the model of Wzb already available in the PDB (Hagelueken *et al.*, 2009). The results obtained will help us towards a better understanding of the regulation of amylovoran biosynthesis modulated by the interplay between AmsA and AmsI, and may possibly help in the design of molecules able to selectively inhibit bacterial tyrosine phosphatases.

Table 3
Data collection and processing.

Values in parentheses are for the outer shell.

Diffraction source	EMBL P13, PETRA III
Wavelength (Å)	1.033
Temperature (K)	100
Detector	PILATUS 6M
Crystal-to-detector distance (mm)	222.6
Rotation range per image (°)	0.1
Total rotation range (°)	360
Exposure time per image (s)	0.1
Space group	$P3_121$
a, *b*, *c* (Å)	66.03, 66.03, 72.27
α, β, γ (°)	90, 90, 120
Mosaicity (°)	0.08
Resolution range (Å)	72.27–1.57 (1.60–1.57)
Total No. of reflections	510981 (25345)
No. of unique reflections	25949 (1253)
Completeness (%)	100 (100)
Multiplicity	19.7 (20.2)
$\langle I/\sigma(I)\rangle$	23.2 (5.5)
$R_{r.i.m.}$†	0.066 (0.598)
Overall *B* factor from Wilson plot ($Å^2$)	16.85

† Estimated by multiplying the conventional R_{merge} value by the factor $[N/(N-1)]^{1/2}$, where *N* is the data multiplicity [R_{merge} = 0.064 (0.583), data multiplicity = 19.7 (20.2)].

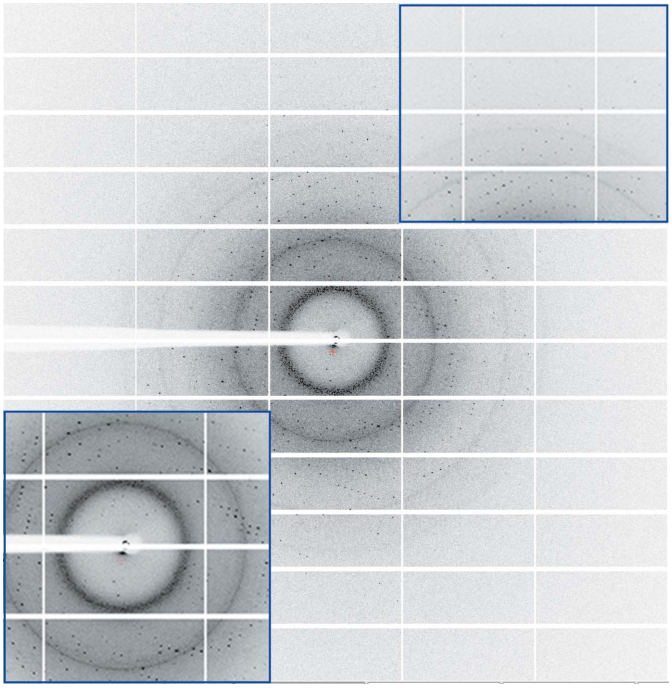

Figure 2
Diffraction image of AmsI collected on a PILATUS 6M detector. The insets show magnifications of the low-resolution and high-resolution regions.

We thank Dr M. Malnoy (Fondazione Edmund Mach, S. Michele all'Adige, Trento, Italy) for providing the genomic DNA from *E. amylovora* strain Ea273. We thank Dr M. Salomone-Stagni for crystal handling at the beamline. Plasmid pETM-11 was obtained from the European Molecular Biology Laboratory under a signed Material Transfer Agreement. Data were collected under European Molecular Biology Laboratory beam time award No. MX-152. This work was supported by the Autonomous Province of Bolzano (project: 'A structural genomics approach for the study of the virulence and pathogenesis of *Erwinia amylovora*').

References

Brzozowski, A. M. & Walton, J. (2001). *J. Appl. Cryst.* **34**, 97–101.
Bugert, P. & Geider, K. (1995). *Mol. Microbiol.* **15**, 917–933.
Bugert, P. & Geider, K. (1997). *FEBS Lett.* **400**, 252–256.
Caputi, L., Cianci, M. & Benini, S. (2013). *Acta Cryst.* F**69**, 570–573.
Caputi, L., Nepogodiev, S. A., Malnoy, M., Rejzek, M., Field, R. A. & Benini, S. (2013). *J. Agric. Food Chem.* **61**, 12265–12273.
Dümmler, A., Lawrence, A.-M. & de Marco, A. (2005). *Microb. Cell Factories*, **4**, 34.
Evans, P. (2006). *Acta Cryst.* D**62**, 72–82.
Evans, P. R. (2011). *Acta Cryst.* D**67**, 282–292.
Geier, G. & Geider, K. (1993). *Physiol. Mol. Plant Pathol.* **42**, 387–404.
Gross, M., Geier, G., Rudolph, K. & Geider, K. (1992). *Physiol. Mol. Plant Pathol.* **40**, 371–381.
Hagelueken, G., Huang, H., Mainprize, I. L., Whitfield, C. & Naismith, J. H. (2009). *J. Mol. Biol.* **392**, 678–688.

Ilan, O., Bloch, Y., Frankel, G., Ullrich, H., Geider, K. & Rosenshine, I. (1999). *EMBO J.* **18**, 3241–3248.
Kabsch, W. (2010). *Acta Cryst.* D**66**, 125–132.
Koczan, J. M., McGrath, M. J., Zhao, Y. & Sundin, G. W. (2009). *Phytopathology*, **99**, 1237–1244.
Langlotz, C., Schollmeyer, M., Coplin, D. L., Nimtz, M. & Geider, K. (2011). *Physiol. Mol. Plant Pathol.* **75**, 163–169.
Lescop, E., Hu, Y., Xu, H., Hu, W., Chen, J., Xia, B. & Jin, C. (2006). *J. Biol. Chem.* **281**, 19570–19577.
Nimtz, M., Mort, A., Domke, T., Wray, V., Zhang, Y., Qiu, F., Coplin, D. & Geider, K. (1996). *Carbohydr. Res.* **287**, 59–76.
Vanneste, J. L. (2000). *Fire Blight: the Disease and its Causative Agent, Erwinia amylovora.* Wallingford: CABI.
Vincent, C., Duclos, B., Grangeasse, C., Vaganay, E., Riberty, M., Cozzone, A. J. & Doublet, P. (2000). *J. Mol. Biol.* **304**, 311–321.
Vrancken, K., Holtappels, M., Schoofs, H., Deckers, T. & Valcke, R. (2013). *Microbiology*, **159**, 823–832.
Wang, D., Korban, S. S., Pusey, P. L. & Zhao, Y. (2011). *Phytopathology*, **101**, 710–717.
Wang, D., Korban, S. S., Pusey, P. L. & Zhao, Y. (2012). *PLoS One*, **7**, e45038.
Wang, D., Korban, S. S. & Zhao, Y. (2009). *Mol. Plant Pathol.* **10**, 277–290.